American J. of Engineering and Applied Sciences 2 (2): 344-352, 2009
ISSN 1941-7020

On the Use of Rolling Element Bearings' Models in Precision Maintenance

Ioannis S. Zotos and Theodore N. Costopoulos
Machine Elements Laboratory, School of Mechanical Engineering,
National Technical University of Athens, Iroon Polytexneiou 9, 15780 Zografou, Greece

Abstract: Problem statement: Rolling element bearings form a very important part of machinery. The increasing demands on their continuous reliable operation under diverse environments make maintenance a very important step towards the efficient use of them. To this end, precision maintenance is a very useful practice, since it deals not only with finding a possible fault of a machine, but also with the identification of its cause and the suggestion of possible preventive measures and corrective actions. In order to better apply precision maintenance techniques though, it is necessary to have a very good insight of the bearings' operation. **Approach:** This study described how the analytical models of the operation of rolling element bearings could be used for the better utilization of precision maintenance in practice. It also presented briefly these analytical models, together with a detailed description of how their results can be used in precision maintenance practice. **Results:** The results of a typical example were given, which showed that the proposed analysis gives an insight of the bearing operation, necessary for the better understanding of the root cause of possible failures. **Conclusion:** This research come to the conclusion that the knowledge of the origin of failures that could be the result of bearing's theoretical models, could be very helpful for the application of precision maintenance practices, since it could lead to the correction of the cause of each failure and thus the bearing will not fail again for the same reason.

Key words: Rolling element bearings, precision maintenance, computer models

INTRODUCTION

The development of analytical models of the operation of rolling element bearings, including loads, stresses and speeds, has been the subject of research of engineers since many years and there exists a big number of very good written documentation on this subject, e.g.,[1].

These models have been used extensively during the initial design stages of new bearings or in demanding applications. Nevertheless, their use as a tool towards better application of precision maintenance practice has not been studied in detail. Apart from that, the interconnections between the working parameters calculated by these models, although apparent and with great importance, have not been examined as much as expected, at least not in published literature or in a form a practitioner would appreciate. On the other end, there are some very analytic investigations of models of rolling element bearings, which try to describe the phenomena up to a very big detail[2-5]. In such cases, although the accuracy achieved is very good, the complexity of the models is such that they cannot be easily applied in everyday maintenance practice.

The aim of this study is to explain how simple mathematical models of rolling element bearings' operation can be used towards the better application of precision maintenance. Also, the importance of understanding and modeling the interconnections between some of the design or operational characteristics of them is pointed out. In order to achieve this aim, an example is presented, regarding the effect of thermal expansion on the load distribution and fatigue life. The equations describing these interconnections are included in a computer program that can be used to create what-if scenarios and better understand the cause of any possible malfunction. The above are performed through analytic equations, introducing all the necessary simplifications, without loosing too much information in the final model, but at the same time keeping the model simple and efficient for everyday maintenance use.

Since there are many combinations of bearing types and loading conditions, it would not be practical to try and cover all of them in this paper. We decided then to include only one of the most representative cases that can give an idea of the method we describe. The selected configuration is a radial ball bearing under

Corresponding Author: Theodore N. Costopoulos, Machine Elements Laboratory, School of Mechanical Engineering, National Technical University of Athens, Iroon Polytexneiou 9, 15780 Zografou, Greece

radial load. Of course the results presented are also applicable to a bigger or smaller extent to other bearing types, since the proposed procedure can be relatively easy extended and adapted to them as well. Apart form that, in order to keep the length of this study short, we consider only bearings turning at moderate speeds and/or not being lightly loaded (so as to be able to ignore centrifugal forces and gyroscopic phenomena). Otherwise these dynamic effects would require far more complicated equations derivations.

MATERIALS AND METHODS

Precision maintenance is based initially on condition monitoring results taken from the bearing under investigation. A malfunction will show up as a characteristic frequency in a vibration spectrum, as an increased shock value in SPM (Shock Pulse Method), as a change in thermal signature in an IR signal, as debris in an oil monitoring system, or as a specific result in any other condition monitoring method. After any of these is present, the machine is scheduled for a stop in order to replace the faulted component. This is the point where precision maintenance procedures start, with the investigation of the cause of the identified failure. Most of the times, it is not easy to identify the cause of a failure, since it could initiate at a different part of the machine, or has its roots even at the design stage of it. For example, even if fatigue seems to be the starting point of a fault, this fatigue could be accelerated or even initiated by the increased loading induced by operation at higher temperatures (thermal expansion), e.g., due to a malfunction in the lubrication system. Without the use of precision maintenance, the faulty bearing would be replaced with a similar one and the fault would reappear after some time. Finding the root cause would lead us to correct the lubrication problem together with the bearing replacement and hence reduce the probabilities of the same fault reappearing for the same reason.

In order to demonstrate a part of the mathematical models built for the precision maintenance of rolling element bearings, we will use the above example and describe the effect of running temperature (and hence thermal expansion) on the load distribution and life of a rolling element bearing under radial load. The interconnections between various phenomena in this case are shown in Fig. 1.

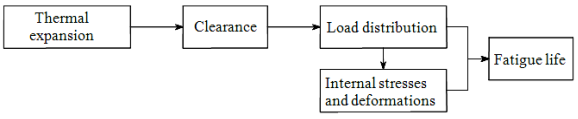

Fig. 1: Interconnections between thermal expansion and fatigue life

Effect of thermal expansion to clearance: As we know, materials expand linearly under the influence of temperature according to the equation:

$$u = \Gamma \cdot L \cdot (T - T_a) \quad (1)$$

Where:
Γ = The coefficient of linear thermal expansion
T_a = The ambient temperature
L = A characteristic length

In the above we have assumed the temperature T to be above the ambient and this is why we use the term expansion. On the contrary, we will have contraction if $T<T_a$. In the following we will use the term expansion, since this is most of the times the case in rolling element bearings in practice. The same equations hold true for contraction as well. In the case of a bearing with outside diameter d_o at temperature T_o-T_a above ambient, the increase in ring outside circumference can be approximated by:

$$u_{toc} = \Gamma_b \cdot \pi \cdot d_o \cdot (T_o - T_a) \quad (2)$$

Hence, the approximate increase in diameter is:

$$u_{to} = \Gamma_b \cdot d_o \cdot (T_o - T_a) \quad (3)$$

The inner ring will undergo a similar expansion given by:

$$u_{ti} = \Gamma_b \cdot d_i \cdot (T_i - T_a) \quad (4)$$

Therefore, the net diametral expansion (change in diametral clearance) will be given by:

$$\Delta_T = \Gamma_b \cdot \left[d_o \cdot (T_o - T_a) - d_i \cdot (T_i - T_a) \right] \quad (5)$$

If the housing is manufactured from a different material than the bearing, then the interference I between the outer ring and the housing may either increase or decrease at elevated temperatures, depending on the coefficients of thermal expansion. The change in interference is:

$$\Delta_{lho} = (\Gamma_b - \Gamma_h) \cdot D_h \cdot (T_o - T_a) \quad (6)$$

Where:
Γ_b and Γ_h = The coefficients of thermal expansion of the bearing and housing respectively
D_h = The initial internal diameter of the housing

If the housing tends to expand more than the bearing, there will be a reduction in interference fit.

A similar procedure can be used for the thermal expansion of the shaft with respect to the bearing, leading to a change of the interference between these two that can be calculated from:

$$\Delta_{Isi} = (\Gamma_s - \Gamma_b) \cdot D_s \cdot (T_i - T_a) \quad (7)$$

Hence finally, the total change in clearance is:

$$\Delta P_d = \Delta_T - \Delta_s - \Delta_h \quad (8)$$

Depending on the magnitude and the sign of ΔT we can finally have an increase or decrease in diametral clearance.

Effect of clearance to the load distribution: Before calculating the load distribution, we show in Fig. 2 the convention followed regarding the angular position ψ of the rolling elements (shown as circles with numbers j).

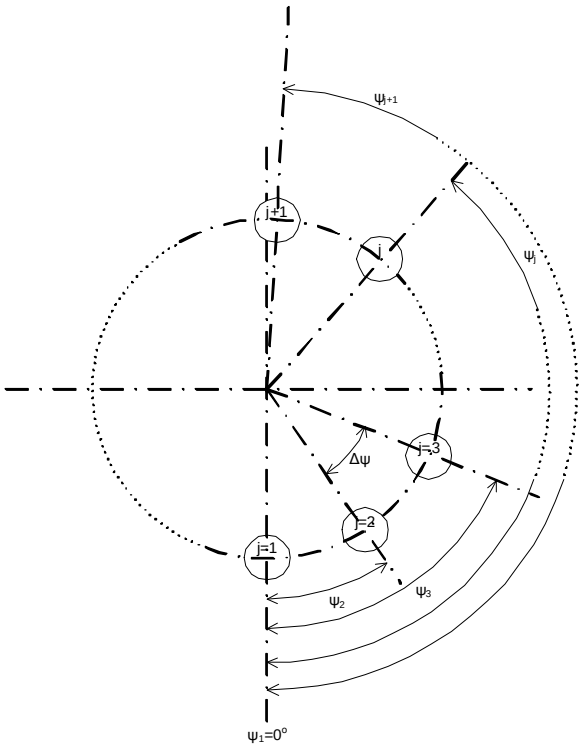

Fig. 2: Angular position convention of rolling elements

According to[1], the equations that must be solved to calculate the static load distribution in a radial ball bearing under radial load are the following:

$$\varepsilon = \frac{1}{2} \cdot \left(1 - \frac{P_d}{2 \cdot \delta_r}\right) \quad (9)$$

$$J_r(\varepsilon) = \frac{1}{2 \cdot \pi} \cdot \int_{-\psi_l}^{+\psi_l} \left[1 - \frac{1}{2 \cdot \varepsilon} \cdot (1 - \cos\psi)\right]^n \cos\psi \cdot d\psi \quad (10)$$

$$F_r = Z \cdot K_n \cdot \left(\delta_r - \frac{1}{2} \cdot P_d\right)^n \cdot J_r(\varepsilon) \quad (11)$$

$$n = \frac{3}{2}, \text{ for ball bearings}$$
$$n = \frac{10}{9}, \text{ for roller bearings} \quad (12)$$

Where:

δ_r = The radial deflection of the bearing ring at $\Psi = 0$
F_r = The applied radial load
Z = The number of rolling elements and
Ψ_1 = The angle defining the loading zone in the bearing ($\pm\Psi_1$ from the zero angle position) given by:

$$\psi_l = \cos^{-1}\left(\frac{P_d}{2 \cdot \delta_r}\right) \quad (13)$$

And K_n is the load-deflection factor, given by:

$$K_n = \left[\frac{1}{\left(1/K_i\right)^{1/n} + \left(1/K_o\right)^{1/n}}\right] \quad (14)$$

where, K_i, K_o are the load-deflection factors for the inner and outer contact respectively. For point contact (e.g., ball bearing) this factor is:

$$K_p = \left|\frac{4}{3} \cdot \sqrt{\frac{2}{\Sigma\rho \cdot (\delta^*)^3}} \frac{E_I \cdot E_{II}}{E_{II} \cdot (\nu_I^2 - 1) + E_I \cdot (\nu_{II}^2 - 1)}\right| \quad (15)$$

In this final equation, E and ν are the Young's modulus and Poisson's ratio of the parts in contact respectively, whereas the dimensionless contact deformation δ* and curvature sum Σρ are given by equations that are presented in the following paragraphs.

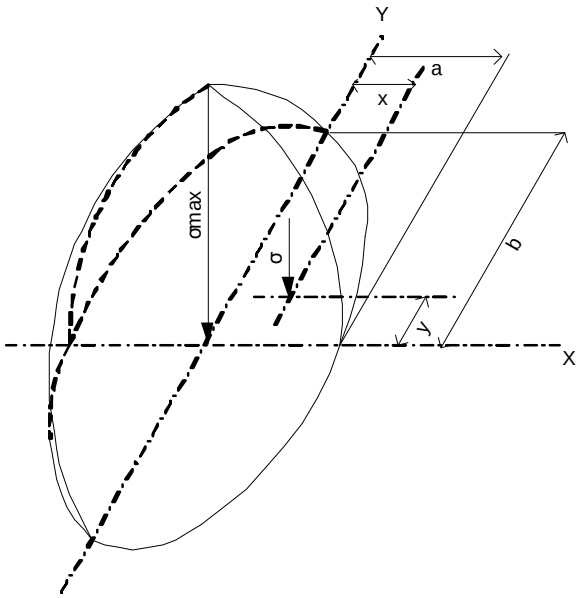

Fig. 3: Compressive stresses in an elliptical contact area

In order now to solve the above equations for δ_r, we have to assume an initial value for δ_r and from that calculate F_r. If this value does not correspond to the real applied F_r, we continue this loop, until we have convergence.

After the calculation of δ_r, we can calculate the maximum load on the rolling elements Q_{max} from the following equation:

$$Q_{max} = K_n \cdot \left(\delta_r - \frac{1}{2}\cdot P_d\right)^n \quad (16)$$

Hence, the load at any rolling element at angle ψ will be:

$$Q_\psi = Q_{max} \cdot \left[1 - \frac{1}{2\cdot\varepsilon}\cdot(1-\cos\psi)\right]^n \quad (17)$$

Effect of load distribution to the internal stresses: The maximum compressive stress in the case of point contact (elliptical contact area), appears at the center of the contact area, as shown in Fig. 3.

The equations calculating the stresses of Fig. 3[1]:

$$\sigma_{max} = \frac{3\cdot Q}{2\cdot\pi\cdot a\cdot b} \quad (18)$$

$$\sigma = \frac{3\cdot Q}{2\cdot\pi\cdot a\cdot b}\cdot\left[1-\left(\frac{x}{a}\right)^2-\left(\frac{y}{b}\right)^2\right]^{1/2} \quad (19)$$

where, Q is the load on the rolling element stemming from the load distribution result and a, b are given by:

$$\alpha = \alpha^*\cdot\left[\frac{3\cdot Q}{2\cdot\Sigma\rho}\cdot\left(\frac{1-\nu_I^2}{E_I}+\frac{1-\nu_{II}^2}{E_{II}}\right)\right]^{1/3} \quad (20)$$

$$b = b^*\cdot\left[\frac{3\cdot Q}{2\cdot\Sigma\rho}\cdot\left(\frac{1-\nu_I^2}{E_I}+\frac{1-\nu_{II}^2}{E_{II}}\right)\right]^{1/3} \quad (21)$$

With I and II referring to the two contacting bodies and:

$$\alpha^* = \left(\frac{2\cdot\kappa^2\cdot\varepsilon}{\pi}\right)^{1/3} \quad (22)$$

$$b^* = \left(\frac{2\cdot\varepsilon}{\pi\cdot\kappa}\right)^{1/3} \quad (23)$$

The corresponding deformation δ is given by the equation:

$$\delta = \delta^*\cdot\left[\frac{3\cdot Q}{2\cdot\Sigma\rho}\cdot\left(\frac{1-\nu_I^2}{E_I}+\frac{1-\nu_{II}^2}{E_{II}}\right)\right]^{2/3}\cdot\frac{\Sigma\rho}{2} \quad (24)$$

where, δ^* is the dimensionless contact deformation given by:

$$\delta^* = \frac{2\cdot f}{\pi}\cdot\left(\frac{\pi}{2\cdot\kappa^2\cdot\varepsilon}\right)^{1/3} \quad (25)$$

And:

$$\kappa = \frac{a}{b} \quad (26)$$

$$\varepsilon = \int_0^{\pi/2}\left[1-\left(1-\frac{1}{\kappa^2}\right)\cdot\sin^2\phi\right]^{1/2} d\phi \quad (27)$$

In order to find κ, we have to interpolate between table values of κ versus $F(\rho) = \frac{(\kappa^2+1)\cdot\varepsilon - 2\cdot f}{(\kappa^2-1)\cdot\varepsilon}$.

The curvature sum $\Sigma\rho$ is given, for inner and outer contacts respectively[1]:

$$\sum\rho_i = \frac{1}{D}\cdot\left(4-\frac{1}{f_i}+\frac{2\cdot\gamma}{1-\gamma}\right) \quad (28)$$

$$\sum\rho_o = \frac{1}{D}\cdot\left(4-\frac{1}{f_o}-\frac{2\cdot\gamma}{1+\gamma}\right) \tag{29}$$

Where:

$$\gamma = \frac{D\cos(\alpha)}{d_m} \tag{30}$$

$$f_i = \frac{r_i}{D}$$
$$f_o = \frac{r_o}{D} \tag{31}$$

In the above, D is the diameter of the rolling elements (balls), a is the contact angle r_i and r_o are the inner and outer groove curvature radii respectively.

In order now to calculate the stresses below the surface, we use the notation of Fig. 4.

According to[1], the equations that must be solved to calculate the subsurface stress field are:

$$S_x = \lambda\cdot\left(\Omega_x + \nu\cdot\Omega_x'\right) \tag{32}$$

$$S_y = \lambda\cdot\left(\Omega_y + \nu\cdot\Omega_y'\right) \tag{33}$$

$$S_z = -\frac{1}{2}\cdot\lambda\cdot\left(\frac{1}{\xi}-\xi\right) \tag{34}$$

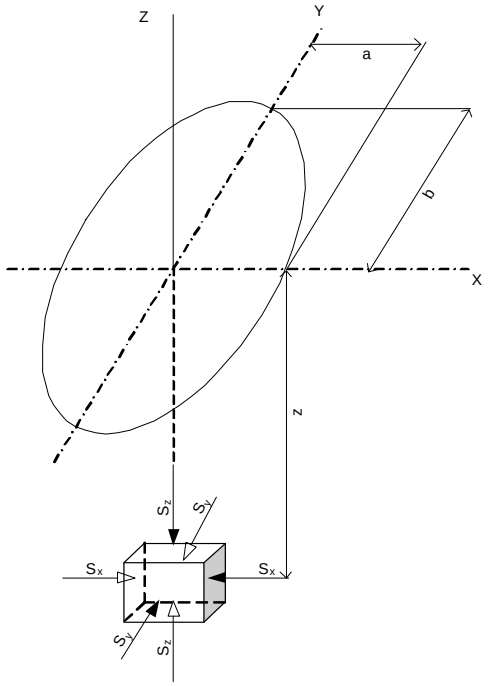

Fig. 4: Stresses below the surface

$$\lambda = \frac{b\cdot\Sigma\rho}{\left(\kappa-\frac{1}{\kappa}\right)\cdot\varepsilon\cdot\left(\frac{1-\nu_I^2}{E_I}+\frac{1-\nu_{II}^2}{E_{II}}\right)} \tag{35}$$

$$\xi = \left(\frac{1+\zeta^2}{\kappa^2+\zeta^2}\right)^{1/2} \tag{36}$$

$$\zeta = \frac{z}{b} \tag{37}$$

$$\Omega_x = -\frac{1}{2}\cdot(1-\xi)+\zeta\cdot\left[f(\phi)-\varepsilon(\phi)\right] \tag{38}$$

$$\Omega_x' = 1-\kappa^2\cdot\xi+\zeta\cdot\left[\kappa^2\cdot\varepsilon(\phi)-f(\phi)\right] \tag{39}$$

$$\Omega_y = \frac{1}{2}\cdot\left(1+\frac{1}{\xi}\right)-\kappa^2\cdot\xi+\zeta\cdot\left[\kappa^2\cdot\varepsilon(\phi)-f(\phi)\right] \tag{40}$$

$$\Omega_y' = -1+\xi+\zeta\cdot\left[f(\phi)-\varepsilon(\phi)\right] \tag{41}$$

$$f(\phi) = \int_0^{\phi}\left[1-\left(1-\frac{1}{\kappa^2}\right)\cdot\sin^2\phi\right]^{-1/2}d\phi \tag{42}$$

$$\varepsilon(\phi) = \int_0^{\phi}\left[1-\left(1-\frac{1}{\kappa^2}\right)\cdot\sin^2\phi\right]^{1/2}d\phi \tag{43}$$

$$\tan^2\phi = t \tag{44}$$

$$\frac{b}{a} = \left[\left(t^2-1\right)\cdot(2t-1)\right]^{1/2} \tag{45}$$

As it is obvious, the above equations can only be solved with the use of a computer.

Effect of the load distribution and the internal stresses to the static and dynamic load capacity of the bearing: In order to see the effects to the dynamic load capacity and life, we use the equations derived in[1], based on the internal stresses and load distribution. We also included most of the simplifications used by Palmgren and Lundberg. This approach leads normally to conservative designs, but since in this study we are interested only on comparative studies (e.g., assessment of reduction of fatigue life due to operational parameters), this will not be a problem.

In brief, the dynamic load capacity (survival after one million cycles) of a point contact is:

$$Q_c = A \cdot \left(\frac{2 \cdot f}{2 \cdot f - 1}\right)^{0.41} \cdot \frac{(1 \mp \gamma)^{1.39}}{(1 \pm \gamma)^{1/3}} \cdot \left(\frac{\gamma}{\cos\alpha}\right)^{0.3} D^{1.8} \cdot Z^{-2/3} \quad (46)$$

The equivalent loading for a rotating ring relative to the load is:

$$Q_{erot} = \left(\frac{1}{2 \cdot \pi} \cdot \int_0^{2\pi} Q_\psi^3 d\psi\right)^{1/3} \quad (47)$$

Whereas for a static ring relative to the load it is:

$$Q_{est} = \left(\frac{1}{2 \cdot \pi} \cdot \int_0^{2\pi} Q_\psi^{10/3} d\psi\right)^{0.3} \quad (48)$$

The dynamic load capacity for the rotating ring is:

$$C_{rot} = Q_{crot} \cdot Z \cdot \frac{J_r}{J_1} \cdot \cos\alpha \quad (49)$$

and for the static ring:

$$C_{st} = Q_{cst} \cdot Z \cdot \frac{J_r}{J_2} \cdot \cos\alpha \quad (50)$$

Applying the multiplication rule for the probabilities (see also reference[1]) we get:

$$C = \left(C_{rot}^{-e} + C_{st}^{-e}\right)^{-1/e} \quad (51)$$

where, $e = \frac{10}{9}$ for point contact.

The life of the bearing will be given by:

$$L_{10} = \left(\frac{C}{F_e}\right)^3 \quad (52)$$

where the equivalent load, for the case where only a radial load is applied, is:

$$F_{er} = \left[\left(\frac{C}{C_{rot}} \cdot \frac{J_r(0.5)}{J_1(0.5)} \cdot \frac{J_1}{J_r}\right)^{3.33} + \left(\frac{C}{C_{st}} \cdot \frac{J_r(0.5)}{J_2(0.5)} \cdot \frac{J_2}{J_r}\right)^{3.33}\right]^{0.3} \cdot F_r \quad (53)$$

Where:

$$J_r' = J_r(\varepsilon = 0.5) \quad (54)$$

$$J_1' = J_1(\varepsilon = 0.5) \quad (55)$$

$$J_2' = J_2(\varepsilon = 0.5) \quad (56)$$

In the above, it is:

$$J_1 = \left\{\frac{1}{2 \cdot \pi} \cdot \int_{-\psi_1}^{\psi_1} \left[1 - \frac{1}{2 \cdot \varepsilon} \cdot (1 - \cos\psi)\right]^{4.5} d\psi\right\}^{1/3} \quad (57)$$

$$J_2 = \left\{\frac{1}{2 \cdot \pi} \cdot \int_{-\psi_1}^{\psi_1} \left[1 - \frac{1}{2 \cdot \varepsilon} \cdot (1 - \cos\psi)\right]^{5} d\psi\right\}^{0.3} \quad (58)$$

RESULTS

Computer program: As it became obvious from the analysis of the previous paragraphs, the equations to be solved for the analysis of this study, are complicated and interconnected and hence can only be solved with the use of a computer program. This computer program was created during the course of the research performed by the authors and its results are presented next. In order to demonstrate the results of the program, we used a 209 single row deep groove ball bearing for which we have detailed geometrical data[1]. The data used for the bearing assembly are shown in Table 1, including both material properties and dimensions.

Effects to the load distribution: In the graphs (Fig. 5a-f), we can see the effect of thermal expansion to the load distribution, namely to the maximum load (Qmax) and to the load zone (psil).

Table 1: Geometrical data of the ball bearing used for demonstration of results

Housing outer diameter (mm)	150
Housing inner diameter (mm)	85
Shaft outer diameter (mm)	45
Shaft inner diameter (mm)	0
Bearing inner contact diameter (mm)	52.291
Bearing outer contact diameter (mm)	77.706
Rolling element diameter (mm)	12.7
Bearing inner groove radius (mm)	6.6
Bearing outer groove radius (mm)	6.6
Number of rolling elements (mm)	9
Bearing contact angle (degrees)	0
Young's modulus of all components (newtonmm^{-2})	200000
Poisson's ratio of all components	0.35
Coefficient of thermal expansion of housing (deg^{-1})	$8.5 \cdot 10^{-6}$ **Titanium
Coefficient of thermal expansion of shaft (deg^{-1})	$8.5 \cdot 10^{-6}$ **Titanium
Coefficient of thermal expansion of outer ring (deg^{-1})	$11.7 \cdot 10^{-6}$ **Steel
Coefficient of thermal expansion of inner ring (deg^{-1})	$11.7 \cdot 10^{-6}$ **Steel
Radial load (Nt)	8900
Inner ring temperature - Ti (deg)	30
Outer ring temperature - To (deg)	50
Ambient (initial) temperature - Ta (deg)	20

From the above we can see that there is an almost linear dependency of both maximum load and load zone with temperature. In every case, we reach a point where there are no further alterations with increased temperature (saturation) and that is when the diametral clearance diminishes.

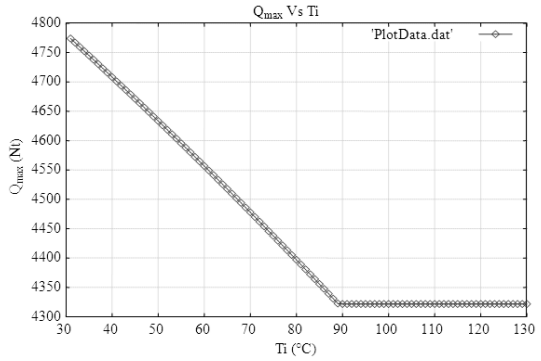

Fig. 5a: Effect of the temperature of the inner ring on the maximum rolling element load

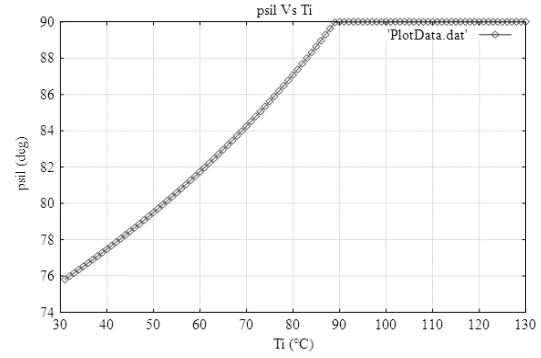

Fig. 5b: Effect of the temperature of the inner ring on the load zone in the bearing

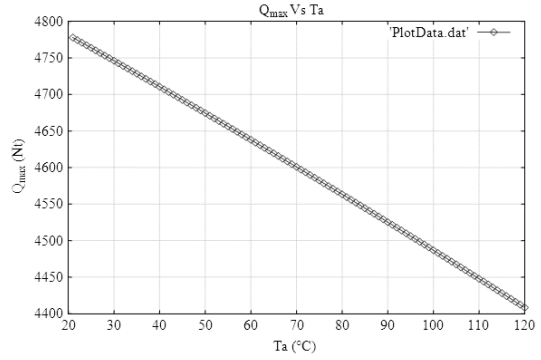

Fig. 5c: Effect of the ambient temperature on the maximum rolling element load

Effects to fatigue life: In the graphs (Fig. 5g-i) we also present the effect of thermal expansion to the fatigue life (L_{10}). It is obvious that temperature has a big influence in life, even ignoring the influence it has in lubricant and material properties. This influence can be used in precision maintenance studies through the application of the proposed model.

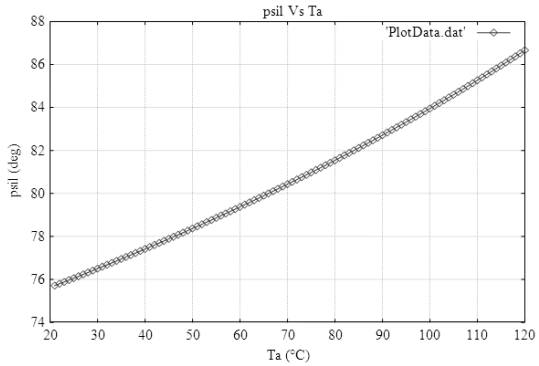

Fig. 5d: Effect of the ambient temperature on the load zone

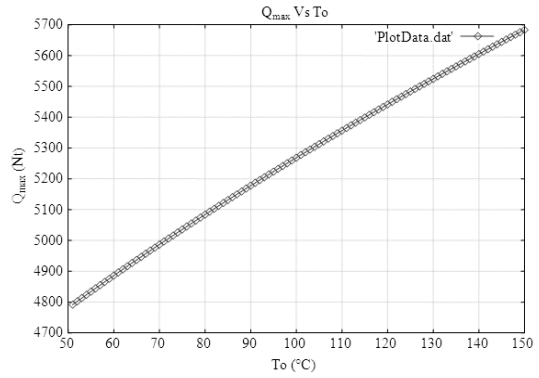

Fig. 5e: Effect of the temperature of the outer ring on the maximum rolling element load

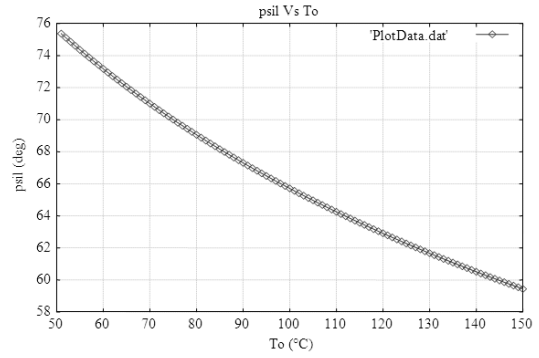

Fig. 5f: Effect of the temperature of the outer ring on the load zone

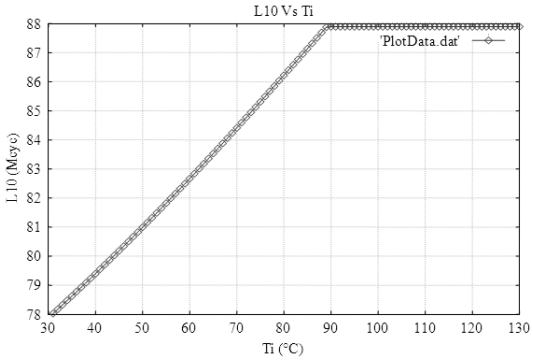

Fig. 5g: Effect of the temperature of the inner ring on the fatigue life

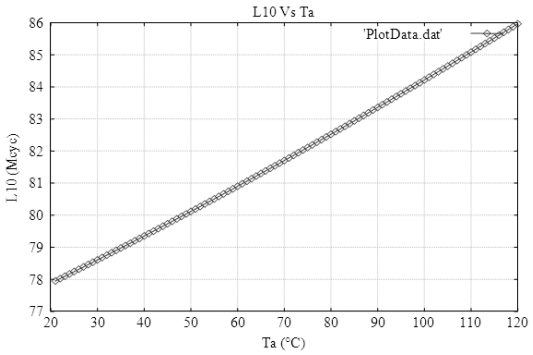

Fig. 5h: Effect of the ambient temperature on the fatigue life

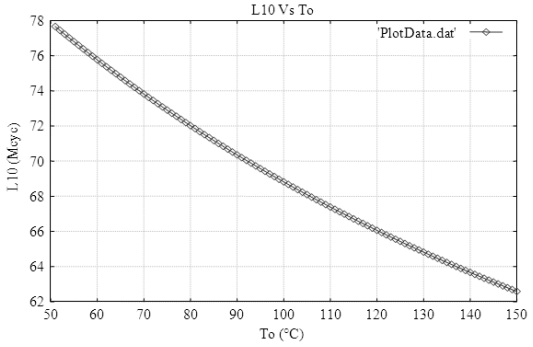

Fig. 5i: Effect of the temperature of the outer ring on the fatigue life

Test rig: In order to validate the conclusions derived from the modeling of various operational characteristics of rolling element bearings, we built a test rig in the Machine Elements Laboratory of the School of Mechanical Engineering in the National Technical University of Athens. A picture of it is shown in Fig. 6.

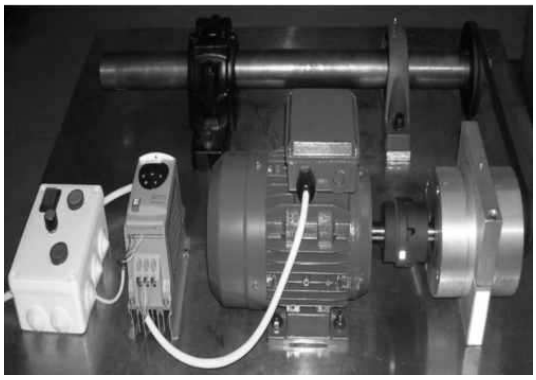

Fig. 6: Test rig picture

This rig contains a number of various rolling element bearings, e.g., in the gearbox or in the driven shaft and it was used to check the validity of the results of our models, as applied to precision maintenance, similar to the model presented in this study. In order to do that and resemble reality as much as possible, a commercial program widely used in practice for preventive maintenance was used. Several faults were introduced in the bearings in order to accelerate the test process and our models were tested against the data recorded during the experiments. In every case, our models could predict qualitatively the possible causes of each introduced fault and their influence in the readings of the instruments. This "qualitative" prediction is anyway what is needed in practice, since we should bare in mind that precision maintenance is partly a science and partly an art and our approach is just a tool that can help the engineer guide his imagination to possible causes and not substitute his/her engineering judgment.

Since the tools used to gather data were the exact ones used in maintenance practice and not sophisticated tailored made solutions, we had available the exact kind of data a maintenance engineer would have. This made our approach to precision maintenance even more realistic and hence the conclusions of our studies more widely accepted.

DISCUSSION

Precision maintenance is a maintenance technique that deals with the correction of the root cause of each fault. Its aim is not just to search for the existence of a fault, but rather to find the reasons behind its appearance. This research presented that the mathematical models of rolling bearings operation can be used as a tool in the search of possible operational

parameters combination that could theoretically lead to failure.

Most of the literature on rolling bearing failures deals with finding the best method to identify a faulty component. This approach leads to the application of predictive maintenance practices, replacing the components based on their condition. This approach though does not deal with the real conditions that lead to this failure, conditions that could initiate from another part of the machine (for example a malfunctioning lubrication pump that leads to an increase of the bearing's operational temperature). That way, the real cause of the failure is not dealt with and thus the same failure can appear again in the future. Using the mathematical models of rolling element bearings as proposed in this research, the real causes of each failure can be searched and appropriate measures taken.

CONCLUSION

This study presents an idea of how analytical models of rolling element bearings can be used in precision maintenance. This is done through the use of an example of a mathematical model of a rolling element bearing. This model gives a clear view of the effects of thermal expansion on the load distribution and fatigue life of a rolling element bearing. The result is that there is a very strong influence and in reality this effect could be even stronger, if we take also into consideration the big influence temperature has in lubricant properties.

The use of the results of this and other similar models in root cause analysis studies can be achieved through the use of what-if scenarios, where we can see how an alteration of a parameter of the model can affect the functional characteristics of a bearing and finally lead to failure. This way, someone can identify and eliminate the cause that lead to the monitored malfunction and thus apply precision maintenance philosophy in practice.

REFERENCES

1. Harris, T.A., 2001. Rolling Bearing Analysis. 4th Edn., John Wiley and Sons, USA., ISBN: 0-471-35457-0.
2. Mack, W. and M. Plöchl, 2000. Transient heating of a rotating elastic-plastic shrink fit. Int. J. Eng. Sci., 38: 921-938, DOI: 10.1016/S0020-7225(99)00064-6
3. Sen, S. and B. Aksakal, 2004. Stress analysis of interference fitted shaft-hub system under transient heat transfer conditions. J. Mater. Des., 25: 407-417. DOI: 10.1016/j.matdes.2003.11.009
4. Sims, P. and R. Zee, 1991. Stress state in turbopump bearing induced by shrink fitting. Proceeding of the AIAA/SAE/ASME/ASEE 27th Joint Propulsion Conference, June 24-26, Sacramento, California, pp: 1-9. http://www.aiaa.org/content.cfm?pageid=406&gTable=mtgpaper&gID=88795
5. Higgins, L.R., 1995. Maintenance Engineering Handbook. 5th Edn., McGraw Hill, New York, USA., ISBN: 0-07-028811-9.